Title

Optical Coherence Tomography of the Larynx: Normative Anatomy and Benign Processes

ISBN

9781493917570

Authors

Sharma, Giriraj K

Wong, Brian J-F

Publication Date

2016

DOI

10.1007/978-1-4939-1758-7_35

Chapter 35

Optical Coherence Tomography of the Larynx: Normative Anatomy and Benign Processes

Giriraj K. Sharma and Brian J.-F. Wong

Introduction

In patients presenting to the otolaryngologist with throat or voice complaints, a comprehensive laryngeal examination is necessary. While no standardized diagnostic workup applies to all laryngology patients, each established technique has advantages and limitations. In the awake, office-based head and neck examination, the most commonly used technique to evaluate the larynx is indirect mirror laryngoscopy. While efficient and least invasive of all examination techniques, this method does not allow for image capture and is limited to a surface view of laryngeal tissues. Flexible fiberoptic or rigid endoscopy with or without videostroboscopy allows for indirect evaluation of the larynx, but is also restricted to a superficial examination of laryngeal lesions. Conventional imaging modalities such as computed tomography (CT), magnetic resonance imaging (MRI), and ultrasound have limited spatial resolution, precluding their ability to characterize subepithelial microanatomy and structural integrity of the vocal folds. Without a precise assessment of depth of penetration and integrity of the basement membrane, surgeons cannot differentiate between benign and malignant lesions of the larynx in patients presenting with identical symptoms. At present, the gold standard for the assessment of malignant processes is microlaryngoscopy with excisional biopsy. This invasive technique is associated with increased healthcare costs, risks of general anesthesia and, most importantly, risk of disruption of vocal fold structure resulting in permanent dysphonia. Hence, there exists a need for a less invasive diagnostic modality which can assess the microanatomy of laryngeal tissues, while preserving the structural integrity of the vocal folds.

Brian J.-F. Wong and Justus Ilgner (eds.), *Biomedical Optics in Otorhinolaryngology: Head and Neck Surgery*,
DOI 10.1007/978-1-4939-1758-7_35,

Anatomy

The layered microstructure of the vocal fold was described by Hirano et al. based on images from a scanning electron microscope [1]. This information formed the basis of the "body-cover" theory of voice production. At the luminal surface, the superficial "cover" consists of stratified squamous epithelium and the superficial (SLP) layer of the lamina propria (LP), as depicted in Fig. 1. Immediately below, the "transition zone" contains the intermediate and deep layers of the LP (combining to form the vocal ligament), while the deeper "body" contains the thyroarytenoid muscle. During phonation, as air flows through the larynx and tension develops within the vocal folds, the contrasting properties of the "cover" and "body" cause a functional separation of these layers and vibration at different rates [1, 2]. Penetrating laryngeal lesions which disrupt the mucosal "cover" or cause tissue loss can disrupt the "body-cover" model, affect VF vibrational parameters, and may lead to significant changes in voice quality.

OCT is capable of characterizing the layered microstructure of the larynx with optical penetration (approximately 1–2 mm) just short of the vocalis muscle. In a cross-sectional image, gray-scale representations of individual tissue layers are based upon their respective backscattering properties. The vocal folds have a weakly scattering epithelium while the SLP, known as Reinke's space, has a loosely organized fibrous composition. Deeper layers of the LP

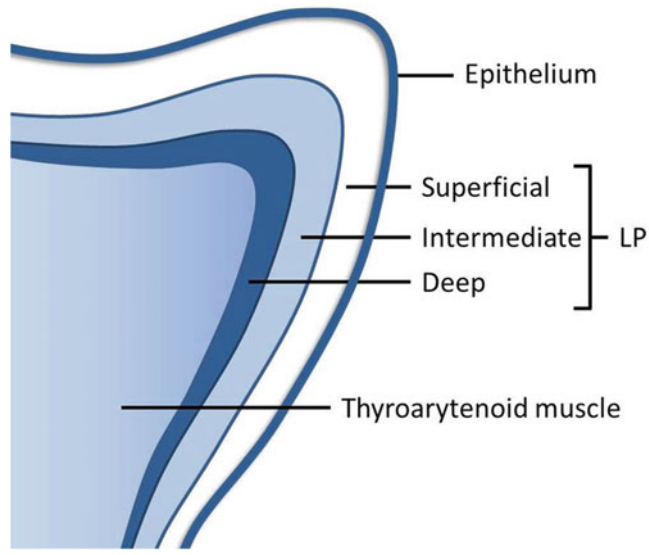

Fig. 1 Cross-sectional schematic of true vocal fold, depicting the epithelium and superficial layer of the lamina propria (LP, "cover"), intermediate and deep layers of the LP ("transition zone"), and the thyroarytenoid muscle ("body")

can be differentiated based on their varying density of collagen and elastic fibers. Hence, OCT can assess depth of penetration of laryngeal lesions and basement membrane and SLP integrity, thus offering a noninvasive means to differentiate benign versus malignant lesions of the larynx.

Principles of OCT

OCT uses a spectrally broadband light source coupled with a low coherence interferometer (e.g., Michelson) to produce high-resolution images of biological tissue. Light from an optical source is split into two arms: a "sample" arm (containing the tissue of interest) and a "reference" arm (stationary or moving mirror). Light back-reflectance from the "sample" is dependent on unique optical backscattering coefficients of biological tissue layers. Both optical paths are recombined and detected to form an interference profile as a function of tissue depth. As the sample beam is scanned across the tissue surface, adjacent depth profiles (A-lines) are compiled to construct two-dimensional or 3-D images with micrometer resolution (~10 μm), millimeter depth (1–2 mm), and video-rate imaging speed [3, 4].

The two principal OCT schemes are time domain OCT (TD-OCT) and frequency or "Fourier" domain OCT (FD-OCT). In 1991, Fujimoto's group published the first report of real-time low coherence tomographic imaging in a biological system [3]. Using a super luminescent diode as a light source, their TD-OCT system used a "reference" beam back-reflected from a moving mirror coupled with a Michelson interferometer to construct an interference pattern. In vitro, cross-sectional images of the retina and coronary artery were produced by mechanically adjusting the distance to the "reference," thereby limiting the image acquisition speed [3]. At the turn of the century, Fercher's group developed the first FD-OCT systems [5, 6]. FD-OCT uses a wavelength-swept light source and with a stationary reference arm to acquire information in the spectral domain, per Fourier transform of the combined spectra at the output of the interferometer. FD-OCT provides improved signal-to-noise ratio, increased image acquisition rates, and higher sensitivity compared to TD-OCT [7–9]. Long-range or "anatomic" OCT (LR-OCT), first pioneered in 2003 by Sampson as a derivative of TD-OCT, and later as version of FD-OCT, extends the axial imaging range of traditional systems without sacrificing resolution [10, 11].

Variations in OCT Technology

Polarization-sensitive OCT (PS-OCT) enhances the diagnostic potential of conventional OCT by recording both the intensity and birefringence of backscattered light. Birefringent tissue (e.g., collagen, muscle, cartilage) changes the polarization state of reflected

light to provide an additional degree of contrast and specificity to fibrous tissue layers. In imaging the vocal folds, increased collagen content in the vocal ligament can be contrasted with the relatively acellular, overlying SLP [12–14]. Furthermore, PS-OCT allows for differentiation between areas of vocal fold scarring and normal epithelium.

In 1993, the first in vivo OCT studies were completed independently by groups at the Massachusetts Institute of Technology (MIT, Boston, MA) and Medical University of Vienna (Vienna, Austria) to image the retina [15, 16]. Later, the introduction of endoscopic OCT systems led to applications in cardiology and gastroenterology [17–21]. Further evolution into ultrahigh-resolution OCT (2–3 μm axial resolution) and spectral domain OCT has expanded the diagnostic potential of OCT within ophthalmology [5, 22–24]. Comprehensive review of OCT principles and research in biomedical interferometry are described in the literature [4, 24, 25].

Evolution of OCT in Laryngology

OCT research within laryngology traverses ex vivo and in vivo imaging in animal and human models. Given the range of applications and imaging techniques (pediatric vs. adult airways, office-based vs. intraoperative imaging, static vs. vibrating vocal folds), OCT systems and optical probe design have evolved to optimize functionality and data quality.

The first systems developed for in vivo scanning of the human larynx utilized near-contact endoscopic probes [19, 26]. These TD-OCT systems (central wavelength $\lambda = 830$ nm, 30 nm bandwidth) integrated the OCT sampling arm into standard endoscopic devices for transverse scanning (30 cm/s) along the plane of laryngeal tissue to identify mucosal structural changes in precancerous and cancerous states. Future iterations of these systems led to the Niris Imaging System (Imalux Corp., Cleveland, OH) which was the only commercially available OCT system for imaging of the upper aerodigestive tract (UADT). Designed as a portable TD-OCT system, this unit includes a 2.7 mm diameter probe to acquire real-time 2D images (200×200 pixels) with a maximum frame rate of 0.7 Hz. The Niris spatial depth resolution is 10–20 μm with scanning depth of 1.5 mm; lateral resolution is 25 μm with lateral scanning range of 1.5–2.5 mm [27]. In 2010, Rubinstein et al. used the Niris system to obtain intraoperative images of normal laryngeal tissue, transition zones, and pathology [27]. A flexible probe held within a modified suction handpiece was inserted through a surgical laryngoscope for controlled, accurate positioning at the area of interest (Fig. 2). The same year, Brenner's group used the Niris system to identify layered tissue microstructure of recurrent respiratory papillomatosis in the trachea [28].

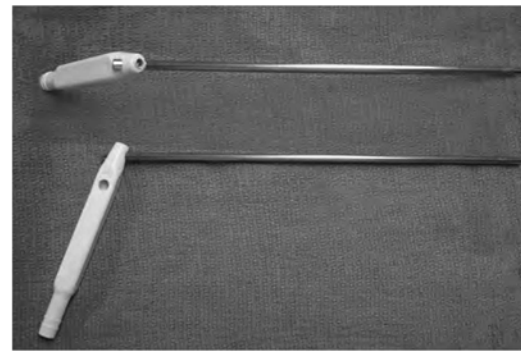

Fig. 2 Specially designed handheld device coupled with NIRIS OCT system to guide a flexible probe into the larynx [27]

At present, most laryngeal imaging has been accomplished using research systems designed and constructed in-house, customized for specific applications of interest. Imaging systems can be adapted for short- or long-range imaging and stationary or rotational scanning. Sampling probe designs may vary in outer diameter, focal length, and direction of light propagation (0° vs 90°).

Ex Vivo Studies

With the advent of faster, minimally invasive OCT systems, research has trended towards in vivo OCT imaging of the human larynx. However, much of our understanding of OCT-based visualization of laryngeal microstructure is derived from studies on harvested tissue. Ex vivo OCT in animal and human models has served to provide anatomical standards for normal laryngeal microanatomy and lay the foundation for OCT-based differentiation of benign versus malignant processes. Furthermore, direct comparison of OCT images with corresponding histological section allows scientists to measure OCT sensitivity and understand limitations associated with the technology and image quality.

Human Studies

In 2004, Bibas et al. used PS-OCT to image 10 tissue samples from a single human postlaryngectomy specimen in both longitudinal (B-scan) and transverse/*en-face* (C-scan) modes. Stacks of C-scans were used to construct 3D images to identify reflectivity patterns within the layered microstructure and to correlate OCT with histological sections [29]. Similarly, de Boer's group used conventional OCT and PS-OCT to image human cadaveric larynges to identify patterns of optical backscattering and tissue birefringence associated with the layered microstructure of normal

laryngeal mucosa [30]. These reports helped to establish standards for OCT-based visualization of laryngeal microanatomy and provided a framework for future OCT data analysis.

Animal Studies

A team led by Luerssen, Lubatschowski, Ptok, and colleagues has been a forerunner in investigating OCT applications in laryngology since the early 2000s. In 2005, Luerssen et al. performed high-resolution TD-OCT (central wavelength $\lambda = 1350$ nm, 5 μm axial resolution) of porcine larynges with an optical fiber tip in direct contact with sample tissue. Their data demonstrated a clear distinction between epithelium and underlying LP, as well as direct correlation of layered microstructure with histologic section [31]. Additional trials by this group in porcine and primate models using high-resolution or fiber-based systems (5–10 μm resolution) in contact mode have been described [32–34]. In these reports, the authors report OCT-based identification of mucosal substructure, laryngeal mucosa micrometry, and comparable sensitivity to histological examination.

Injury to laryngeal mucosa secondary to gastroesophageal reflux, prolonged endotracheal intubation, or laser therapy for VF lesions triggers a wound healing cascade which, if undiagnosed, terminates in granulation and fibrosis. However, occult subepithelial pathology cannot be identified by operative endoscopy or CT/MRI. Multiple ex vivo animal studies have demonstrated OCT capability of identifying laryngeal and subglottic histopathology following simulated morphologic injury to the VF or subglottis [35–37]. Karamzadeh et al. studied OCT of a variety of simulated subglottic injuries (collagen injection, dehydration, rehydration/edema, and repeated intubation) in harvested rabbit larynges [35]. Larynges were suspended vertically in an OCT imaging stage with a probe positioned over the cricoid cartilage to acquire images vertically, in a cephalocaudal direction. OCT-based micrometry of mucosal tissues demonstrated an increase in LP thickness following submucosal injury, as well as unique signal intensity patterns correlating with levels of subepithelial collagen or edema [35].

Operative treatment of glottic lesions is often limited by the surgeon's inability to precisely gauge the depth of disease. Given the critical interaction of adjacent layers of the laryngeal mucosa during phonation, the "body cover" model must be respected during excision of glottic lesions to prevent vocal fold scarring or permanent dysphonia. In 2007, Wisweh et al. performed simultaneous OCT and femtosecond laser (fs-laser) cutting on extracted porcine larynges [38]. An OCT system developed by Optimec Ltd. (Nizhny Novgorod, Russia) with 15 μm spatial resolution was used to identify sites of therapy and provides a reference for positioning the sample; the OCT scanner was swiveled out prior to fs-laser ablation at defined volumes and depths. This was the first report which investigated the potential of OCT as an intraoperative imaging tool to guide laryngeal microsurgery.

Clinical Studies

Intraoperative Imaging

In the operative setting, the larynx is exposed under direct laryngoscopy and visualized with an operating microscope and flexible or rigid endoscope (0°–90°). Intraoperative OCT of the larynx has been studied using a flexible endoscopic probe or a probe integrated with an operative microscope. In 1997, Sergeev et al. reported the first in vivo imaging of the larynx. Under direct laryngoscopy, a flexible sampling arm was advanced through the working channel of a standard endoscope and positioned 5–7 mm away from the tissue of interest. The distal fiber tip was swung by a galvanometric plate to image healthy laryngeal tissue and differentiate epithelium and LP based on optical scattering properties [19].

In 2005, Wong et al. reported laryngeal OCT during surgical endoscopy in 82 patients using a custom-built handheld probe. A flexible sampling fiber encased in a transparent, flexible plastic sheath was supported by an outer metal tube (2 mm diameter) and manually guided through the laryngoscope for near-contact or gentle contact imaging of laryngeal mucosa (axial resolution 9 μm, depth 2.6 mm). Images were analyzed for epithelial thickness, layered structure of the mucosa, and microstructural features (e.g., glands, microvasculature). Benign pathology, including Reinke's edema, papillomatosis, polyps, mucous cysts, and granulation tissue were identified based on unique patterns of signal backscattering [39]. In 2008, Kraft et al. used a commercial, contact-mode OCT device (Optimec Ltd.; central wavelength $\lambda = 980$ nm, 15 μm spatial resolution) to compare the diagnostic accuracy of microlaryngoscopy with OCT compared with microlaryngoscopy alone in a series of 217 benign and malignant laryngeal lesions [40]. They found that microlaryngoscopy and OCT provided an accurate diagnosis in 93 % of benign lesions and had a higher sensitivity (78 %) than microlaryngoscopy alone (66 %) in predicting epithelial dysplasia; specificity and accuracy were comparable in both methods.

Additional reports on OCT under direct laryngoscopy or microlaryngoscopy have been described [27, 40–46]. Later, spectral domain systems boasting faster imaging speeds (up to 18.5 frames/s) demonstrated improved efficiency and allow for 3D endoscopic imaging [47]. While imaging through endoscope working channels or handheld probes allow for contact or near-contact imaging, certain factors have been found to limit image quality. Motion artifact due to the movement of the probe tip, enhanced by surgeon's hand tremor, can significantly affect OCT image quality given its high-resolution scale. Furthermore, placement of a probe within the laryngoscope limits the surgeon's visualization of the operative field and interferes with insertion and manipulation of microlaryngeal instruments [48]. To answer this challenge, Vokes et al. first described a hands-free noncontact OCT system, with the

sampling probe integrated with a surgical microscope. They integrated a custom built TD-OCT system with a novel interface device attached to an operating microscope by acrylic housing. The interface device consisted of a lens to adjust the focal length of the OCT beam, a galvanometer-mounted mirror to allow for coronal scanning and a second fixed mirror to redirect the path of light towards the sample tissue. Image frames were acquired at 1.6 mm depth and 6 mm width, with axial resolution of approximately 7 μm [48]. Additional reports of OCT integrated with microlaryngoscopy have been described in the literature [49, 50].

Office-Based Imaging

OCT probes can be affixed to flexible or rigid endoscopes to perform awake, office-based laryngeal imaging. Conjoining the sampling arm with a flexible endoscope allows for imaging (contact or near-contact) with a fixed working distance from the vocal folds, easier manipulation of the instrument, and a side-view of the vocal cords. However, direct contact with the vocal folds may precipitate severe cough, gagging or, in rare cases, laryngospasm. In rigid endoscopes cantilevered in the oropharynx approximately 5–8 cm above the vocal folds, LR-OCT systems can scan the larynx in a less invasive manner which may be better tolerated by patients. However, this method requires manual adjustment of the working distance with any movement.

In 2005, Luerssen et al. first described laryngeal OCT in awake patients under local anesthesia. A fiber-based endoscopic system (Institute of Applied Physics, Nizhny Novgorod, Russia) acquired images with the distal end of the sampling probe (2 mm diameter) in direct contact with laryngeal tissues. OCT data demonstrated clear distinction between epithelial mucosa and the loose, subepithelial collagenous tissue of the LP [31]. Additional studies by Luerssen's group describe a laryngoscope-integrated OCT probe for noncontact, transoral imaging with a low-profile design to optimize practicality and patient comfort [32–34]. Figure 3 demonstrates OCT images from healthy false vocal folds (supraglottic tissues), acquired from a research system (Fig. 3a) and a commercially available system (Fig. 3b). This data demonstrates respiratory epithelium, consisting of pseudostratified columnar epithelium with mucous-secreting goblet cells and ciliae. In contrast, OCT of the healthy true vocal folds depict nonkeratinized, stratified squamous epithelium (Fig. 4).

Chen and Wong's group constructed a TD-OCT system with a sampling probe fixed onto a laryngoscope to perform transoral, noncontact OCT [51]. This first-generation system had a slow scanning mechanism (1 frame/s) and produced images with significant motion artifact secondary to patient movement (breathing, swallowing, and reflexes) and physician hand tremor. Later, the same research group developed an FD-OCT system with a "double barrel" handheld carriage integrating a gradient-index (GRIN) lens-based probe

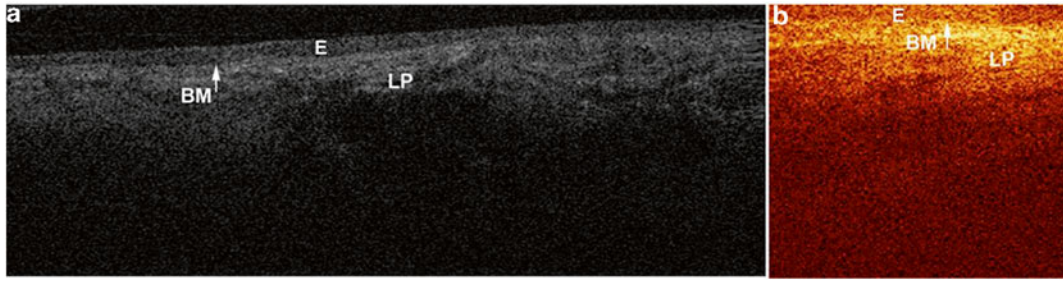

Fig. 3 OCT images of the normal false vocal folds acquired from a research OCT system (**a**) and a commercially available OCT system (**b**). *E* Epithelium (psuedostratified columnar), *BM* basement membrane locus, *LP* lamina propria

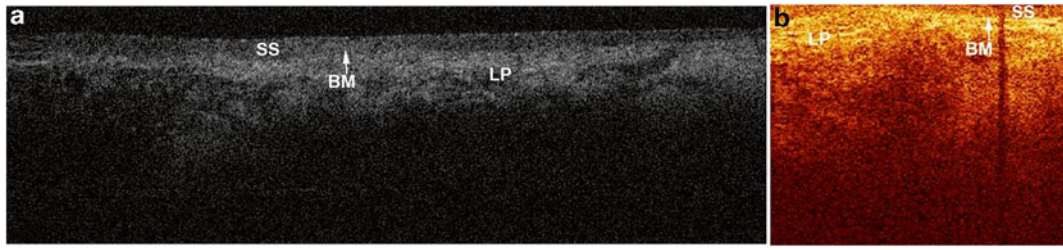

Fig. 4 OCT images of the normal true vocal fold acquired from a research OCT system (**a**) and a commercially available OCT system (**b**). *SS* stratified squamous epithelium, *BM* basement membrane locus, *LP* lamina propria

and rigid video endoscope. This instrument acquired cross-sectional images at 8 frames/s, thus reducing the degree of motion artifact [52]. Further pushing the frontier in dynamic imaging of the VF, a swept source (central wavelength $\lambda = 1310$ nm) FD-OCT system was designed (Fig. 5a) and constructed to acquire transoral endoscopic images of the larynx at 40 frames/s using an enhanced long GRIN lens-based probe integrated with a rigid endoscope in a similar double-barrel apparatus (Fig. 5b) [53]. Lubatschowski's group integrated a swept-source FD-OCT system with a rigid laryngoscope for noncontact OCT and synchronous video imaging of the vocal folds through a singular beam path [54]. Their compact imaging apparatus offered a more practical and well-tolerated means for transoral office-based imaging of the vocal folds. These noncontact, transoral endoscopic systems were the first to provide synchronous OCT and video imaging of the larynx during respiration and phonation without the use of topical anesthesia. Furthermore, noncontact imaging prevents morphometric distortion which may result from direct tissue compression from the tip of the probe. Awake, office-based OCT offers comparable results to contact or near-contact OCT during surgical endoscopy, however, with lower axial resolution (20 μm). Limitations of these modified laryngoscope-based systems include

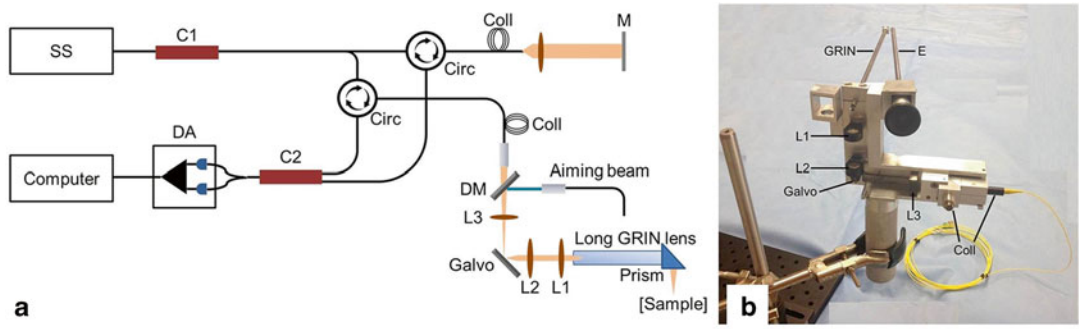

Fig. 5 Schematic diagram of gradient index (GRIN) lens rod-based dynamic focusing swept-source OCT system (**a**). Handheld "double barrel" carriage with integrated OCT probe and rigid endoscope for transoral imaging of the larynx. *SS* swept light source (central wavelength $\lambda = 1310$ nm), *C1* 1×2 coupler, *C2* 2×2 coupler, *DA* differential amplifier, *Circ* circulator, *Coll* collimator, *DM* dichotic mirror, *L1*, *L2* lenses (coupled with GRIN lens to form an optical ballast and produce an optical relay within the reference arm), *L3* focusing lens, *Galvo* galvanometer, *M* mirror, *E* rigid endoscope

motion artifact caused by patient movement during the exam (e.g., breathing, swallowing, reflexes) and physician's hand tremor. Furthermore, because the endoscope-OCT systems were cantilevered within the limited space of the pharynx, an extended focal length (compared to systems integrated with surgical endoscopes) was required for laryngeal imaging, limiting the lateral resolution and signal intensity [31, 32, 51, 55]. Currently, long-range swept source systems are being designed for high-speed transoral imaging without compromise of resolution.

In 2006, Klein et al. described laryngeal OCT and PS-OCT in awake subjects using a probe integrated with a flexible transnasal endoscope. The OCT probe, encased in Teflon tubing, was advanced through the operating channel of the endoscope until the distal end was visible and placed in contact with the glottic mucosal surface. Images were analyzed for epithelial micrometry, gray-scale intensity variation secondary to birefringent tissue (i.e., collagen content), and unique features of benign processes (e.g., papilloma, cysts, scarring) [41]. Additional reports of awake, office-based, flexible endoscopic OCT are described in the literature [56].

Vocal Fold Vibration

Vocal fold vibration has been widely studied under normal and pathologic circumstances using laryngeal videostroboscopy and high-speed video. Lohscheller et al. utilized phonovibrography to translate vocal fold vibration frequency, velocity, and acceleration into 2D diagrams for visualization and analysis [57, 58]. In examination of patients with laryngeal lesions, clinicians routinely correlate endoscopic findings with characteristics of vocal fold

vibration noted on stroboscopy. This information helps to predict the consequence of lesions or interventions on phonation. However, the diagnostic sensitivity and specificity of endoscopy with videostroboscopy is low, as examination is limited to a surface view of the vocal folds. Thus, noninvasive diagnostic technology is needed to characterize the laryngeal mucosal wave in 3D during phonation. Correlation of high-resolution cross-sectional OCT images with vibratory characteristics of the laryngeal mucosa (e.g., frequency, amplitude) may lead to better understanding of how lesions or interventions affect the mechanical properties of laryngeal mucosal tissue and alter phonation.

In 2006, Luerssen's group first reported in vivo TD-OCT (central wavelength $\lambda = 1300$ nm) of the vocal folds during phonation [32]. A fiber-based OCT probe was integrated into a beam path of a laryngoscope to capture images in noncontact mode with a scanning rate of 10 Hz (resolution 10–20 μm). By measuring oscillation peaks in relation to scanning time, they were able to calculate vibrational frequency. Later, Yu et al. used a swept-source FD-OCT system to image vocal fold oscillation at 40 frames/s [53]. The higher frame rate allowed for minimization of motion artifact and dynamic vibration of the vocal folds. In seated, nonanesthetized patients, an OCT probe attached to a laryngoscope was inserted through the oral cavity and centered above the larynx. Their device allowed for dual-channel endoscopic and video-rate OCT imaging of the vocal folds. In both studies, vibration parameters such as frequency and amplitude were calculated from individual OCT frames. In 2011, Wong and Chen's group demonstrated OCT and optical Doppler tomography (ODT) of vibrating focal folds using a swept-source FD-OCT system (center wavelength $\lambda = 1050$ nm) with an imaging speed of 100 frames/s [59]. Their system extended the limit for high-speed functional OCT with image frames rate near that of physiologic fundamental frequencies (females 200 Hz, males 120 Hz).

Typically, however, imaging speeds of OCT systems are insufficient to directly capture vocal fold oscillation in the audio frequency range. To answer this challenge, Chang et al. reported motion-triggered laser scanning to capture four-dimensional (4D) images of vibrating ex vivo calf larynges [60]. Their modified OCT system acquired multiple A-lines over a single oscillation cycle at a frequency of 100 Hz before shifting to the adjacent transverse location. This method of data acquisition allows for temporal and spatial registration of A-lines to yield phase-aligned snapshots of tissue oscillation over a complete vibratory cycle. Hence, the imaging frequency range is determined by the A-line rate (up to 200 kHz) instead of the OCT system frame rate. Additional studies of triggered laser scanning of vibrating laryngeal tissue are reported in the literature [61].

Neonatology and Pediatrics

Anatomy

The neonatal and adult larynges differ significantly in both structural and microanatomic aspects. In the newborn airway, the larynx sits higher up and more anteriorly while the circumferential cricoid results in a cross-sectional narrowing of the airway at the subglottis [62]. Newborn VF mucosa consists of a uniform, monolayered LP composed of ground substances (hyaluronic acid, fibronectin, fibroblasts, collagenous and elastic fibers), less fibrous components, and no vocal ligament [63]. During the adolescent years, the LP matures into a layered microstructure. The delicate mucosa of the newborn larynx, coupled with the unique anatomical configuration of the airway, make the newborn laryngeal and subglottic tissues susceptible to injury following long-term intubation or gastroesophageal reflux.

Boseley et al. used pediatric cadaveric larynges to describe the maturation of the vocal fold. They noted a differentiation from the monolayered LP into a bilaminar structure beginning by 2 months of age. Transition into a trilaminar structure occurs between ages 1 and 5 years, with full maturation into the adult molecular composition occurring around age 13 [64]. However, it is unknown exactly when these transitions occur and thus difficult to estimate at what age microsurgical techniques can be used without affecting phonation. OCT's ability to evaluate the subepithelial microstructure of the pediatric larynx can allow clinicians to assess stage of laryngeal development and develop individualized treatment plans.

Future Applications

Given the unique anatomical configuration of the neonatal airway, patients requiring long-term endotracheal intubation and mechanical ventilation are at risk for subglottic mucosal injury. In managing neonates with suspected subglottic stenosis, pediatric otolaryngologists do not have means to comprehensively evaluate the airway without subjecting patients to general anesthesia and further airway instrumentation. Direct laryngoscopy and bronchoscopy is the gold standard for diagnosis of SGS [65]. However, this procedure may lead to further mucosal abrasion (removal and reinsertion of endotracheal tube, endoscope contact with airway mucosa) and is limited to a view of surface anatomy. Furthermore, risks of general anesthesia in patients with preexisting cardiopulmonary insufficiencies must be considered. These factors, combined, often lead to a delay in diagnosis of SGS and increased morbidity. Thus, there exists a need for a less invasive imaging modality which can characterize the subepithelial tissue of the subglottis and identify precursors to subglottic stenosis.

OCT Studies

In 2007, Ridgway et al. were the first to use OCT to image the pediatric upper aerodigestive tract. Using a fiber-based OCT system, they imaged 15 pediatric patients during operative endoscopy

at various airway landmarks with a flexible, handheld probe positioned manually or with endoscopic guidance. Layered microstructure of normal laryngeal and subglottic tissue and distinct pathologic changes (mature scar, granulation tissue, edema, ulceration) were identified on OCT and correlated with endoscopic photographs [66]. The following year, the same group conducted in vivo OCT of the larynx in intubated neonates to identify tissue microstructure of the larynx, subglottis, and proximal trachea. This data provided a framework for using OCT to identify subepithelial injury at the subglottis in neonates under long-term intubation [67].

Boudoux et al. conducted ex vivo imaging of both pediatric and porcine larynges using FD-OCT, spectrally encoded confocal microscopy, and full-field optical coherence microscopy followed by comparison with histologic section. They noted that the combined application of OCT with confocal microscopy allows for comprehensive evaluation of subepithelial microstructure and cellular and subcellular components of the vocal folds. Combined, these modalities may allow for longitudinal analysis of vocal fold development and differentiation [68, 69].

OCT Limitations

The primary limitation of OCT imaging of the larynx is the depth of signal penetration. Current OCT systems offer optical penetration depths of up to 1–2 mm. As benign and malignant processes are differentiated by depth of invasion and disruption of the basement membrane, achieving adequate signal penetration is critical to providing a definitive diagnosis of laryngeal pathology. Larger, exophytic lesions of greater than 2 mm depth cannot be identified to their full extent, limiting the diagnostic sensitivity of OCT. Furthermore, certain tissue interfaces (e.g., cartilage, bone) with high optical scattering or absorption properties impede photon penetration and cast a distal shadow within A-lines, further limiting diagnostic sensitivity in such tissues. Additional factors which limit image quality include physician hand tremor and patient movement during office-based OCT, or equipment vibrations which may all translate into image distortion of far greater magnitude. Lastly, the OCT resolution limit (approximately 10 μm) precludes evaluation of laryngeal microanatomy at the cellular level. This degree of microanatomical analysis is fundamental for differentiation between dysplastic, precancerous, and cancerous lesions, necessitating formal histopathologic analysis for a definitive diagnosis of malignancy.

At present, near-contact sampling probes offer the best OCT image resolution, clarity, and diagnostic sensitivity. This method of imaging requires general anesthesia for OCT under microlaryngoscopy or adequate topical anesthesia for awake, office-based laryngeal OCT. However, office-based near-contact imaging may

not be well tolerated by all patients, given the risk of paroxysmal airway reactions such as coughing, gagging, or choking. While these reactions may be self-limiting and the incidence of true laryngospasm is rare, noncontact imaging may cause discomfort or anxiety to some patients. Current efforts are focused on developing full range OCT systems using vertical-cavity surface-emitting lasers (VCSEL), which may ultimately allow for transoral imaging of the vocal cords from a sampling arm cantilevered in the oropharynx while maintaining current spatial resolution.

Malignancy

OCT has been shown to provide detailed microanatomical information about the laryngeal epithelial layer and integrity of the BM and LP [29–31]. By identification of small foci of BM breakdown, OCT can identify premalignant or invasive cancerous lesions with high sensitivity [70, 71]. In 1997, Sergeev et al. were the first to study normal and cancerous tissue of the larynx and reported a "loss of normal tissue stratification in tumors" [19]. Later, Shakhov et al. conducted TD-OCT in 26 patients with small laryngeal squamous cell carcinomas. Similarly, they described a stratification of layered tissue within mucosa of the healthy larynx, the disappearance of which signifies pathologic changes [26]. Further OCT studies on premalignant and malignant lesions of the larynx are illustrated and reviewed elsewhere in this text [39, 43, 70].

References

1. Hirano M. Morphological structure of the vocal cord as a vibrator and its variations. Folia Phoniatr (Basel). 1974;26(2):89–94.
2. Titze IR, Jiang J, Drucker DG. Preliminaries to the body-cover theory of pitch control. J Voice. 1988;1(4):314–9.
3. Huang D, et al. Optical coherence tomography. Science. 1991;254(5035):1178–81.
4. Fercher AF. Optical coherence tomography—development, principles, applications. Z Med Phys. 2010;20(4):251–76.
5. Fercher AF, et al. Measurement of intraocular distances by backscattering spectral interferometry. Opt Commun. 1995;117:43–8.
6. Wojtkowski M, et al. In vivo human retinal imaging by Fourier domain optical coherence tomography. J Biomed Opt. 2002;7(3):457–63.
7. Beaurepaire E, et al. Full-field optical coherence microscopy. Opt Lett. 1998;23(4):244–6.
8. Yun S, et al. High-speed optical frequency-domain imaging. Opt Express. 2003;11(22):2953–63.
9. Choma M, et al. Sensitivity advantage of swept source and Fourier domain optical coherence tomography. Opt Express. 2003;11(18):2183–9.
10. Armstrong J, et al. In vivo size and shape measurement of the human upper airway using endoscopic longrange optical coherence tomography. Opt Express. 2003;11(15):1817–26.
11. Jing J, et al. High-speed upper-airway imaging using full-range optical coherence tomography. J Biomed Opt. 2012;17(11):110507.
12. de Boer JF, et al. Two-dimensional birefringence imaging in biological tissue by polarization-sensitive optical coherence tomography. Opt Lett. 1997;22(12):934–6.
13. de Boer JF, Milner TE. Review of polarization sensitive optical coherence tomography and Stokes vector determination. J Biomed Opt. 2002;7(3):359–71.
14. Kuo WC, et al. Polarization-sensitive optical coherence tomography for imaging human atherosclerosis. Appl Opt. 2007;46(13):2520–7.

15. Fercher AF, et al. In vivo optical coherence tomography. Am J Ophthalmol. 1993;116(1): 113–4.
16. Swanson EA, et al. In vivo retinal imaging by optical coherence tomography. Opt Lett. 1993;18(21):1864–6.
17. Tearney GJ, et al. Scanning single-mode fiber optic catheter-endoscope for optical coherence tomography. Opt Lett. 1996;21(7):543–5.
18. Tearney GJ, et al. In vivo endoscopic optical biopsy with optical coherence tomography. Science. 1997;276(5321):2037–9.
19. Sergeev A, et al. In vivo endoscopic OCT imaging of precancer and cancer states of human mucosa. Opt Express. 1997;1(13):432–40.
20. de Feyter PJ, Nieman K. New coronary imaging techniques: what to expect? Heart. 2002;87(3):195–7.
21. Sivak Jr MV, et al. High-resolution endoscopic imaging of the GI tract using optical coherence tomography. Gastrointest Endosc. 2000;51(4 Pt 1):474–9.
22. Drexler W. Ultrahigh-resolution optical coherence tomography. J Biomed Opt. 2004;9(1): 47–74.
23. Drexler W, et al. In vivo ultrahigh-resolution optical coherence tomography. Opt Lett. 1999;24(17):1221–3.
24. Yaqoob Z, Wu J, Yang C. Spectral domain optical coherence tomography: a better OCT imaging strategy. Biotechniques. 2005;39(6 Suppl):S6–13.
25. Drexler W, Fujimoto JG. In: Drexler W, Fujimoto JG, editors. Introduction to Optical Coherence Tomography Optical coherence tomography: technology and applications. New York: Springer; 2008; 1–45.
26. Shakhov AV, et al. Optical coherence tomography monitoring for laser surgery of laryngeal carcinoma. J Surg Oncol. 2001;77(4):253–8.
27. Rubinstein M, et al. Optical coherence tomography of the larynx using the Niris system. J Otolaryngol Head Neck Surg. 2010; 39(2):150–6.
28. Colt HG, et al. Multimodality bronchoscopic imaging of recurrent respiratory papillomatosis. Laryngoscope. 2010;120(3):468–72.
29. Bibas AG, et al. 3-D optical coherence tomography of the laryngeal mucosa. Clin Otolaryngol Allied Sci. 2004;29(6):713–20.
30. Burns JA, et al. Imaging the mucosa of the human vocal fold with optical coherence tomography. Ann Otol Rhinol Laryngol. 2005;114(9):671–6.
31. Luerssen K, et al. Optical characterization of vocal folds with optical coherence tomography. Photon Ther Diagn. 2005;5686:328–32.
32. Lurssen K, et al. Optical characterization of vocal folds using optical coherence tomography—art. no. 60781O. Photon Ther Diagn II. 2006;6078:O781.
33. Lurssen K, et al. Optical coherence tomography in the diagnosis of vocal folds. HNO. 2006;54(8):611–5.
34. Lueerssen K, et al. Optical characterization of vocal folds by OCT-based laryngoscopy—art. no. 64241O. Photon Ther Diagn III. 2007;6424:O4241.
35. Karamzadeh AM, et al. Characterization of submucosal lesions using optical coherence tomography in the rabbit subglottis. Arch Otolaryngol Head Neck Surg. 2005;131(6): 499–504.
36. Nassif NA, et al. Measurement of morphologic changes induced by trauma with the use of coherence tomography in porcine vocal cords. Otolaryngol Head Neck Surg. 2005;133(6): 845–50.
37. Torkian BA, et al. Noninvasive measurement of ablation crater size and thermal injury after CO2 laser in the vocal cord with optical coherence tomography. Otolaryngol Head Neck Surg. 2006;134(1):86–91.
38. Wisweh H, et al. Optical coherence tomography monitoring of vocal fold femtosecond laser microsurgery—art. no. 663207. Ther Laser Appl Laser-Tissue Interact III. 2007; 6632:63207.
39. Wong BJ, et al. In vivo optical coherence tomography of the human larynx: normative and benign pathology in 82 patients. Laryngoscope. 2005;115(11):1904–11.
40. Kraft M, et al. Clinical value of optical coherence tomography in laryngology. Head Neck. 2008;30(12):1628–35.
41. Klein AM, et al. Imaging the human vocal folds in vivo with optical coherence tomography: a preliminary experience. Ann Otol Rhinol Laryngol. 2006;115(4):277–84.
42. Foster MC, et al. Association of subcutaneous and visceral adiposity with albuminuria: the Framingham Heart Study. Obesity (Silver Spring). 2011;19(6):1284–9.
43. Kraft M, et al. Significance of optical coherence tomography in the assessment of laryngeal lesions—art. no. 68421O. Photon Ther Diagn IV. 2008;6842:O8421.
44. Zhu Y, et al. Discovery and characterization of sulfoxaflor, a novel insecticide targeting sapfeeding pests. J Agric Food Chem. 2011; 59(7):2950–7.
45. Lima LH, et al. A new dual port cutter system for vitrectomy surgery. Retina. 2010;30(9): 1515–9.

46. Norwood KW, et al. Traumatic brain injury in children and adolescents: surveillance for pituitary dysfunction. Clin Pediatr (Phila). 2010;49(11):1044–9.
47. Kim KH, et al. In vivo 3D human vocal fold imaging with polarization sensitive optical coherence tomography and a MEMS scanning catheter. Opt Express. 2010;18(14): 14644–53.
48. Walker SE, et al. Racial/ethnic discrepancies in the metabolic syndrome begin in childhood and persist after adjustment for environmental factors. Nutr Metab Cardiovasc Dis. 2012;22(2): 141–8.
49. Wilhelm-Leen ER, et al. Vitamin D deficiency and frailty in older Americans. J Intern Med. 2010;268(2):171–80.
50. Krishnamoorthy G, et al. Electrokinetic lab-on-a-biochip for multi-ligand/multi-analyte biosensing. Anal Chem. 2010;82(10): 4145–50.
51. Guo S, et al. Office-based optical coherence tomographic imaging of human vocal cords. J Biomed Opt. 2006;11(3):30501.
52. Guo S, et al. Gradient-index lens rod based probe for office-based optical coherence tomography of the human larynx. J Biomed Opt. 2009;14(1):014017.
53. Yu L, et al. Office-based dynamic imaging of vocal cords in awake patients with swept-source optical coherence tomography. J Biomed Opt. 2009;14(6):064020.
54. Wisweh H, et al. A laryngoscope for office-based imaging of human vocal folds using OCT. Proc SPIE. 2009;7372.
55. Easter B, et al. The impact of music on the PACU patient's perception of discomfort. J Perianesth Nurs. 2010;25(2):79–87.
56. Sepehr A, et al. Optical coherence tomography of the larynx in the awake patient. Otolaryngol Head Neck Surg. 2008;138(4):425–9.
57. Lohscheller J, et al. Phonovibrography: mapping high-speed movies of vocal fold vibrations into 2-D diagrams for visualizing and analyzing the underlying laryngeal dynamics. IEEE Trans Med Imaging. 2008;27(3):300–9.
58. Lohscheller J, Eysholdt U. Phonovibrogram visualization of entire vocal fold dynamics. Laryngoscope. 2008;118(4):753–8.
59. Liu G, et al. Imaging vibrating vocal folds with a high speed 1050 nm swept source OCT and ODT. Opt Express. 2011;19(12):11880–9.
60. Chang EW, Kobler JB, Yun SH. Triggered optical coherence tomography for capturing rapid periodic motion. Sci Rep. 2011;1:48.
61. Kobler JB, et al. Dynamic imaging of vocal fold oscillation with four-dimensional optical coherence tomography. Laryngoscope. 2010;120(7): 1354–62.
62. Holinger PH, et al. Subglottic stenosis in infants and children. Ann Otol Rhinol Laryngol. 1976;85(5 Pt.1):591–9.
63. Sato K, Hirano M, Nakashima T. Fine structure of the human newborn and infant vocal fold mucosae. Ann Otol Rhinol Laryngol. 2001;110(5 Pt 1):417–24.
64. Boseley ME, Hartnick CJ. Development of the human true vocal fold: depth of cell layers and quantifying cell types within the lamina propria. Ann Otol Rhinol Laryngol. 2006; 115(10):784–8.
65. Holinger LD. Diagnostic endoscopy of the pediatric airway. Laryngoscope. 1989;99(3):346–8.
66. Ridgway JM, et al. Imaging of the pediatric airway using optical coherence tomography. Laryngoscope. 2007;117(12):2206–12.
67. Ridgway JM, et al. Optical coherence tomography of the newborn airway. Ann Otol Rhinol Laryngol. 2008;117(5):327–34.
68. Boudoux C, et al. Optical microscopy of the pediatric vocal fold. Arch Otolaryngol Head Neck Surg. 2009;135(1):53–64.
69. Boudoux C, et al. Preliminary evaluation of noninvasive microscopic imaging techniques for the study of vocal fold development. J Voice. 2009;23(3):269–76.
70. Armstrong WB, et al. Optical coherence tomography of laryngeal cancer. Laryngoscope. 2006;116(7):1107–13.
71. Hughes OR, et al. Optical and molecular techniques to identify tumor margins within the larynx. Head Neck. 2010;32(11):1544–53.